

This discussion paper is/has been under review for the journal Natural Hazards and Earth System Sciences (NHESD). Please refer to the corresponding final paper in NHESD if available.

Dominant processes of extreme rainfall-producing mesoscale convective system over southeastern Korea: 7 July 2009 case

J.-H. Jeong¹, D.-I. Lee², C.-C. Wang³, and I.-S. Han⁴

¹Radar Analysis Division, Weather Radar Center, KMA, Seoul, Republic of Korea

²Department of Environmental Atmospheric Sciences, Pukyong National University, Busan, Republic of Korea

³Department of Earth Sciences, National Taiwan Normal University, Taipei, Taiwan

⁴Fishery and Ocean Information Division, National Institute of Fisheries Science, Busan, Republic of Korea

Received: 17 September 2015 – Accepted: 13 October 2015 – Published: 28 October 2015

Correspondence to: D.-I. Lee (leedi@pknu.ac.kr)

Published by Copernicus Publications on behalf of the European Geosciences Union.

NHESD

3, 6459–6489, 2015

Dominant processes of extreme rainfall-producing mesoscale convective system

J.-H. Jeong et al.

Title Page

Abstract

Introduction

Conclusions

References

Tables

Figures

⏪

⏩

◀

▶

Back

Close

Full Screen / Esc

Printer-friendly Version

Interactive Discussion

Abstract

An extreme rainfall-producing mesoscale convective system (MCS) associated with the Changma front in southeastern Korea was investigated using observational data. This event recorded historic rainfall and led to devastating flash floods and landslides in the Busan metropolitan area on 7 July 2009. The aim of the present study is to analyze and better understand the synoptic and mesoscale environment, and the behavior of quasi-stationary MCS causing extreme rainfall. Synoptic and mesoscale analyses indicate that the MCS and heavy rainfall occurred association with a stationary front which resembled a warm front in structure. A strong southwesterly low-level jet (LLJ) transported warm and humid air and supplied the moisture toward the front, and the air rose upwards above the frontal surface. As the moist air was conditionally unstable, repeated upstream initiation of deep convection by back-building occurred at the coastline, while old cells moved downstream parallel to the convective line with training effect. Because the motion of convective cells nearly opposed the backward propagation, the system as a whole moved slowly. The back-building behavior was linked to the convectively produced cold pool and its outflow boundary, which played an essential role in the propagation and maintenance of the rainfall system. As a result, the quasi-stationary MCS caused a prolonged duration of heavy rainfall, leading to extreme rainfall over the Busan metropolitan area.

1 Introduction

Extreme rainfall often endangers public health and safety, and causes significant economic losses worldwide. In particular, damages caused by these events in metropolitan areas are especially serious due to large and dense populations. Certain atmospheric conditions (or structures) are required for extreme rainfall events to occur; these include synoptic and mesoscale features such as typhoons, synoptic disturbances (lows and fronts), summer monsoonal flow, and mesoscale convective systems (MCSs). Among

Dominant processes of extreme rainfall-producing mesoscale convective system

J.-H. Jeong et al.

[Title Page](#)

[Abstract](#)

[Introduction](#)

[Conclusions](#)

[References](#)

[Tables](#)

[Figures](#)

[⏪](#)

[⏩](#)

[◀](#)

[▶](#)

[Back](#)

[Close](#)

[Full Screen / Esc](#)

[Printer-friendly Version](#)

[Interactive Discussion](#)



record since 1905 at the Busan station. Thus, this rainfall event was climatologically extreme and rare for Busan.

One unique aspect of this historic heavy rainfall event was its localized nature over the southeastern Korean Peninsula. Figure 2a shows the rainfall distribution for 7 July 2009 over Korea, an area over 300 km in length and 200 km in width. The daily rainfall accumulation exceeding 150 mm was concentrated within a narrow east–west oriented band over the southern Korean Peninsula and rainfall greater than 300 mm was confined to the southeastern corner of the peninsula. The time series of hourly rainfall at three stations in this narrow heavy rainfall region (> 150 mm) are plotted in Fig. 2b–d. Rain rates > 30 mm h⁻¹ are of shorter duration at Gwangju and Masan (Fig. 2b and c) compared with Busan (Fig. 2d) station, where the heavy rainfall persisted for longer as the result of a slow-moving MCS, or of the sustained regeneration of convection.

To investigate the mechanisms leading to the extreme rainfall in Busan, the results of our analysis on this quasi-stationary MCS and the heavy-rainfall event on the southeastern Korean Peninsula are presented here. In the current paper, we seek to answer the following specific questions using observational analysis: how does the synoptic and mesoscale environment influence the quasi-stationary MCS, and what processes supported heavy rainfall in Busan area.

1.2 Organization of paper

The following sections analyze the extreme rainfall-producing MCS on 7 July 2009. The data and methodology are presented in Sect. 2, and Sect. 3 described the synoptic and thermodynamic environment. Section 4 discusses the evolution and structure of the quasi-stationary MCS, which led to extreme rainfall over the over the Busan metropolitan area. Section 5 provides further discussion, and finally Sect. 6 gives a concluding summary.

Dominant processes of extreme rainfall-producing mesoscale convective system

J.-H. Jeong et al.

[Title Page](#)

[Abstract](#)

[Introduction](#)

[Conclusions](#)

[References](#)

[Tables](#)

[Figures](#)

[⏪](#)

[⏩](#)

[◀](#)

[▶](#)

[Back](#)

[Close](#)

[Full Screen / Esc](#)

[Printer-friendly Version](#)

[Interactive Discussion](#)



2 Data and methodology

The multiscale analysis in the present study draws on a variety of observational and model-based datasets. The National Centers for Environmental Prediction–National Center for Atmospheric Research (NCEP–NCAR) global reanalysis dataset (6 hourly) with $2.5^\circ \times 2.5^\circ$ horizontal resolution and 17 vertical levels (Kalnay et al., 1996) was used for the discussion of synoptic conditions. Some mesoscale charts and diagnostics were generated using the Japan Meteorological Agency mesoscale spectrum model (JMA-MSM) analysis at a horizontal resolution of 5 km at 16 levels (Saito et al., 2006) every 3 h (at 00:00, 03:00, 06:00, and 09:00 LST) on 7 July 2009. The lack of available soundings in southern Korea and its vicinity unfortunately precludes a detailed depiction of the atmosphere thermodynamics and kinematics upstream from the quasi-stationary MCS over Busan. Thus, some alternative sounding and domain-averaged information for this event was taken from the JMA-MSM analysis. Furthermore, hourly infrared (IR) images from the Multi-functional Transport Satellite (MTSAT) obtained from the Weather Satellite Image Archive, Kochi University, were used to examine the overall distribution of convection. These images have a grid spacing of 0.05° in both longitude and latitude.

To document the detailed structures of the quasi-stationary MCS, ground-based Doppler radar observations and surface data were used. The radar data were obtained from the operational S-band (10 cm) Doppler radar of the Korea Meteorological Administration (KMA) installed in Busan (PSN, 35.12° N, 129° E). The Doppler radar, covering a radius of 250 km in the southeastern Korean Peninsula, performed a volume scan every 10 min at 13 elevation angles ($0.01, 0.2, 0.6, 1.0, 1.4, 1.9, 2.8, 4.0, 5.5, 7.4, 9.6, 12.3, \text{ and } 15.6^\circ$). The Doppler radar data were interpolated onto a Cartesian coordinate system with vertical and horizontal grid intervals of 0.25 and 1 km, respectively. A Cressman-type weighting function was used for the interpolation (Cressman, 1959). Surface observations received from collected sites of the Automatic Weather System (AWS) operated by the KMA, which have a 1 min time update resolution, were ana-

Dominant processes of extreme rainfall-producing mesoscale convective system

J.-H. Jeong et al.

[Title Page](#)

[Abstract](#)

[Introduction](#)

[Conclusions](#)

[References](#)

[Tables](#)

[Figures](#)

[⏪](#)

[⏩](#)

[◀](#)

[▶](#)

[Back](#)

[Close](#)

[Full Screen / Esc](#)

[Printer-friendly Version](#)

[Interactive Discussion](#)

lyzed to investigate the time series and accumulated amount of rainfall, and variations of surface temperature and wind.

3 Synoptic and thermodynamic environment

3.1 Synoptic environment

5 The manually analyzed surface weather maps for 7 July 2009 with satellite IR brightness temperature (T_B) superimposed are presented in Fig. 3 to reveal the synoptic conditions under which the MCS developed. At 03:00 LST, the Changma front west of 127° E was oriented roughly east–west and extended into eastern China along about 35° N (Fig. 3a). While meso- α scale (Orlanski, 1975) MCSs also existed south of the front and over eastern China (Ninomiya and Akiyama, 1992), deep convection with $T_B \leq 220$ K developed along and slightly to the north of the surface Changma front near southwestern Korean Peninsula.

15 Six hours later at 09:00 LST (00:00 UTC), the front had moved forwards slightly but had become more wavy; the surface low pressure became well defined west of Korea and propagated toward the northeast (Fig. 3b). The convection over southwestern Korea redeveloped vigorously, and had expended in size area north of the front. At this time, the organized MCS was moving across the southern Korean Peninsula and producing heavy rainfall up to more than 200 mm per day. Deep convection over south-eastern Korea seen in the T_B imagery persisted for more than 9 h over the exact same region (cf. Fig. 2a).

20 The NCEP–NCAR reanalysis at 09:00 LST 7 July at the surface indicates a strong geopotential height gradient between the subtropical high and the deepening frontal low (Fig. 4a). Associated with this, strong monsoonal southwesterly low-level flow existed with clear confluence between the deepening low and the anticyclonic flow along the perimeter of the subtropical high. At 850 hPa (Fig. 4b), a southwesterly flow of $\geq 15 \text{ m s}^{-1}$ also appeared, with speeds clearly exceeding the 12.5 m s^{-1} criterion often

Dominant processes of extreme rainfall-producing mesoscale convective system

J.-H. Jeong et al.

[Title Page](#)

[Abstract](#)

[Introduction](#)

[Conclusions](#)

[References](#)

[Tables](#)

[Figures](#)

[⏪](#)

[⏩](#)

[◀](#)

[▶](#)

[Back](#)

[Close](#)

[Full Screen / Esc](#)

[Printer-friendly Version](#)

[Interactive Discussion](#)



Dominant processes of extreme rainfall-producing mesoscale convective system

J.-H. Jeong et al.

[Title Page](#)

[Abstract](#)

[Introduction](#)

[Conclusions](#)

[References](#)

[Tables](#)

[Figures](#)

[⏪](#)

[⏩](#)

[◀](#)

[▶](#)

[Back](#)

[Close](#)

[Full Screen / Esc](#)

[Printer-friendly Version](#)

[Interactive Discussion](#)

air from the East China Sea toward the front, where strong convergence was evident. At 06:00 LST (Fig. 5c), the front over southern Korea had become more wavy with intensified low pressure. Three hours later (09:00 LST, Fig. 5d), the Changma front over southern Korea became apparently distorted, which resulted from faster eastward frontal movement on the west side and slower movement over the southeastern coast of Korea. The flow deceleration over southeastern Korea resulted in at the sharp horizontal temperature contrast across the surface front, with clearly colder. The air behind (north of) the Changma front (e.g. Li et al., 1997). Moreover, the θ_e gradient steepened further near the coastline ahead of southeastern Korea during the heavy rainfall in Busan. Physically, the advection of θ_e is important because it represents the advection of both warm air and moisture. The warm air advection at low levels can be lined synoptic-scale ascent through the quasi-geostrophic omega equation (Bluestein, 1992), and it can increase the atmospheric instability (i.e. increase the vertical temperature lapse rate) as well.

The vertical cross sections across the Changma front along transect A–B (33° N, 128° E to 38° N, 131° E) are plotted to investigate the vertical structure of the front, moisture advection and wind distribution. Associated strong θ_e gradients, the frontal boundary resembles the characteristics of a warm front at low levels (Fig. 6). The warm and moist air extends northward and glides up above the surface front. The upward motion ($3\text{--}5\text{ ms}^{-1}$) near the prefrontal zone continues up to 800 hPa. The main area of widespread precipitation is produced by the ascent of the southwesterly flow (warm air advection) of moist air above the baroclinic (frontal) zone. This transport of warm and moist air to greater heights increases the amount of water that can be condensed and precipitated. On the other hand, a relatively cold and dry region appears to the north of the surface front underneath the frontal slope. Relatively weak downward motion ($1\text{--}3\text{ ms}^{-1}$) was generally present over this region in the lower troposphere, which suggests that the MCS developed on the cool side of the frontal boundary. Due to the evaporation of precipitation below the frontal zone, the air there can rapidly moisten and become saturated. At 06:00 LST, a well-mixed structure (near 342 K) appeared

from 900 to 600 hPa due to heavy rainfall over southeastern Korea (Fig. 6b). This is consistent with satellite observations, which show that MCS was located behind the surface frontal boundary (Fig. 3).

3.3 Upstream thermodynamic environment

5 In the vertical cross sections above, some important aspects of the upstream oncoming flow associated with convective instability in the LLJ are also clearly depicted. The thermodynamic profile at 34° N, 128.5° E (marked by an asterisk in Fig. 5c) about 120 km upstream from the quasi-stationary MCS, derived from the JMA-MSM analysis at 03:00 LST 7 July 2009, indicates conditional instability for a surface air parcel, with
10 a convective available potential energy (CAPE) of 283 J kg⁻¹ and negligible convective inhibition (CIN; 9 J kg⁻¹, not shown). Mainly as a result of low-level warm air advection over the ocean, the CAPE increased to about 764 J kg⁻¹ at 09:00 LST (Fig. 7) within 6 h. The temperature lapse rate indicated conditional instability below 300 hPa. The lifting condensation level (LCL) showed quite low at 981 hPa, and the level of free
15 convection (LFC) is also low at 943 hPa. It is due to high moisture advection through deep layers. The 0–3 km wind velocity difference was about 7.7 ms⁻¹ and equivalent to a bulk shear (BS) of $6.6 \times 10^{-3} \text{ s}^{-1}$. These wind velocity and BS were comparable to Meiyu frontal precipitation systems (Wang et al., 2011). From 600 to 200 hPa, the winds turned into westerly with maximum wind speed about 23 ms⁻¹ at 200 hPa. Dur-
20 ing 00:00–03:00 LST, there was a significant increase in low-level southwesterly flow below 3 km (not shown). This phenomenon will be shown to be linked to the movement of the quasi-stationary MCS over southeastern Korea, and will be further elaborated upon in Sect. 4.

Dominant processes of extreme rainfall-producing mesoscale convective system

J.-H. Jeong et al.

[Title Page](#)

[Abstract](#)

[Introduction](#)

[Conclusions](#)

[References](#)

[Tables](#)

[Figures](#)

[⏪](#)

[⏩](#)

[◀](#)

[▶](#)

[Back](#)

[Close](#)

[Full Screen / Esc](#)

[Printer-friendly Version](#)

[Interactive Discussion](#)



4 Structure and evolution of the quasi-stationary MCS

4.1 Overview of the quasi-stationary MCS

The PSN radar constant altitude point position indicator (CAPPI) of reflectivity display at 2 km altitude from volume-scans during 06:00–09:00 LST on 7 July 2009 (Fig. 8) depicts the meso- β scale structure and evolution of MCS responsible for the heavy rainfall in Busan. By 06:00 LST, a group of quasi-discrete cells had formed, embedded within a larger area of precipitation near the Busan metropolitan area (Fig. 8a). With time, the convection became organized into a linear shape along the coastline and expanded in size and intensity as it evolved into a squall line with deep convection at its leading edge by 07:00 LST (Fig. 8b). At this time, an area of stratiform precipitation was present behind the leading convective line, which was oriented northeast–southwest and approximately 120 km long. Convective cells in excess of 40 dBZ were embedded within this quasi-stationary squall line. As old cells moved slowly northeastward, new cells formed to the southwest and merged into the line, while the whole MCS remained quasi-stationary (Fig. 8c). At 08:00 LST, the squall line continued to narrow and its middle segment bulged forward. The bowl-like feature expanded at 09:00 LST (Fig. 8d), but the convective line was over the same region as three hours earlier and had hardly moved.

On the basis of the radar reflectivity distribution, the MCS was characterized by a “leading-line trailing-stratiform (TS)” organizational mode (Houze et al., 1990; Parker and Johnson, 2000; Schumacher and Johnson, 2005). TS–MCSs are often associated with a synoptic cold front, but in this case developed north of a warm front. The environment in the present case obviously differs from that in previous studies.

A more detailed description of the structure of the extreme rainfall-producing MCS at 10 min intervals from 07:00 to 07:20 LST 7 July 2009 is given by Fig. 9. A leading convective line (≥ 40 dBZ) appeared along the coast of Busan with northeast–southwest alignment (Fig. 9) and moved slowly northeastward. At 07:10 LST, a new convective cell (reflectivity values ≥ 47 dBZ) was initiated on the upstream side (rear flank) of the con-

[Title Page](#)

[Abstract](#)

[Introduction](#)

[Conclusions](#)

[References](#)

[Tables](#)

[Figures](#)

[⏪](#)

[⏩](#)

[◀](#)

[▶](#)

[Back](#)

[Close](#)

[Full Screen / Esc](#)

[Printer-friendly Version](#)

[Interactive Discussion](#)



**Dominant processes
of extreme
rainfall-producing
mesoscale
convective system**

J.-H. Jeong et al.

[Title Page](#)[Abstract](#)[Introduction](#)[Conclusions](#)[References](#)[Tables](#)[Figures](#)[|◀](#)[▶|](#)[◀](#)[▶](#)[Back](#)[Close](#)[Full Screen / Esc](#)[Printer-friendly Version](#)[Interactive Discussion](#)

prevailed in the lower troposphere especially below 2 km and turned gradually into westerly flow at upper levels. The 0–3 km wind velocity difference was about 8.2 m s^{-1} , equivalent to a BS of $6.8 \times 10^{-3} \text{ s}^{-1}$. The tropospheric winds generally veered with height, with a roughly reverse shear direction aloft. Strong shear reversal has been documented in back-building MCS events by Schumacher and Johnson (2008).

Corfidi et al. (1996) and Corfidi (2003) developed a simple vector technique to predict MCS motion using advection and propagation. The propagation component is defined as the rate of change of location of new cell development relative to existing cells (Chappell, 1986; Doswell et al., 1996). They reported that the mean motion of the cells comprising the convective system is highly correlated with the mean 850–300 hPa wind. The convective cells in our case clearly moved in the direction of the mid-level wind (above 5 km). The cell-motion vector is from about 230° at 9 m s^{-1} (Fig. 11), while the mid-level mean wind direction is approximately 229° (16 m s^{-1}) between 3 and 7 km. This is consistent with the results from previous studies. The propagation vector (forward 225° , 7 m s^{-1}) was generally oriented opposite to the mean wind and cell motion. The individual cells moved northeastward parallel to the convective line, but back-building propagation was southwestward, resulting in a system movement that was slowly northeastward or quasi-stationary. The convective system moved slowly from 240° at 4 m s^{-1} and to the right of the mean wind. This slow system motion can be explained by a “cancellation” or near cancellation of the cell motion and backward propagation vectors, as described by Chappell (1986). Hence, the present case clearly included: (i) the movement of convective cells opposing the motion from backward propagation, (ii) convective cells moving parallel to the convective line, (iii) the system as a whole moving slowly. This produces a persistent convective event at a given location.

5 Discussion

The previous section explained how the quasi-stationary MCS can be characterized in terms of a back-building process and that is an important mechanism leading to extreme rainfall in the Busan metropolitan area. To understand why convective initiation could occur continuously upstream (southwest flank) of system, we will examine how preexisting mesoscale features influence the system, and how the system itself can alter the inflow environment and feedback changes in the system-scale structure and longevity. Recall that the primary features of the mesoscale system during heavy rainfall were associated with a surface warm front. The quasi-stationary MCS formed on the well-defined synoptic-to-meso- α scale frontal boundary (see Fig. 5). Figure 12 presents the time–height section of areal-mean horizontal wind and θ_e over the same domain as in Fig. 11. The strong monsoonal southwesterly LLJ near the quasi-stationary MCS appeared from 06:00 LST 7 July 2009. During this period, the strength of the MCS tends to coincide with the LLJ intensity, as also seen earlier in mesoscale and radar analysis. It suggests that the LLJ can play a role in the development of convection (i.e. Trier et al., 2006; Wang et al., 2012; Jeong et al., 2012, 2013). The southwesterly LLJ influenced deep convection by enhancing warm advection in the frontal zone. Additionally, air with high θ_e is advected over a stationary frontal boundary by the LLJ between 03:00 and 06:00 LST 7 July. Junker et al. (1999) also found that a maximum of positive θ_e advection is typically located near the rainfall maximum. It follows that continued strengthening of the southwesterly LLJ would feed the development of convection in the vicinity of Busan.

Many studies of linear-convective-system-like squall lines have suggested the importance of lower-tropospheric line-perpendicular shear (e.g. Rotunno et al., 1998; Weisman and Rotunno, 2004). However, this event occurred with line-parallel vertical shear in the lower troposphere (Fig. 12). During 05:00–06:00 LST, the region of relatively cool surface temperature ($\leq 20^\circ\text{C}$) gradually expanded, and thus the cold pools formed from previous precipitation progressed northeastward in the direction of convective system

[Title Page](#)

[Abstract](#)

[Introduction](#)

[Conclusions](#)

[References](#)

[Tables](#)

[Figures](#)

[⏪](#)

[⏩](#)

[◀](#)

[▶](#)

[Back](#)

[Close](#)

[Full Screen / Esc](#)

[Printer-friendly Version](#)

[Interactive Discussion](#)



**Dominant processes
of extreme
rainfall-producing
mesoscale
convective system**

J.-H. Jeong et al.

[Title Page](#)[Abstract](#)[Introduction](#)[Conclusions](#)[References](#)[Tables](#)[Figures](#)[⏪](#)[⏩](#)[◀](#)[▶](#)[Back](#)[Close](#)[Full Screen / Esc](#)[Printer-friendly Version](#)[Interactive Discussion](#)

movement (Fig. 13a and b). With the arrival of the cold pools at the coastline, the surface temperature depression was approximately 3–5 °C (Fig. 13c and d). The elongated surface cold pools formed along the convective line, nearly parallel to the axis of convection in terms of radar reflectivity field (Figs. 8b and 13c). By 08:00 LST, the cold pools remained the same location while the convective line moved quite slowly. It appeared that the role of the cold pools for propagation of the convective line may be important. The dominant role of the cold pools will be discussed and confirmed through sensitivity experiments in future works. In addition, a sudden change in surface wind direction and speed was observed in southern Busan at 06:00 LST (marked by the box in Fig. 13b). Relatively strong southwesterly and northeasterly converge along the outflow boundary (marked dashed line in Fig. 13b–d) on the southeastern periphery of the convective line. The northeasterly wind with downdraft-driven cold air and the southwesterly with warm moist air are evident within the outflow boundary (Fig. 13b–d). New convective cells are initiated at the cold outflow boundaries and then organized into the southwest–northeast oriented convective band in the warm inflow region to the south (Figs. 8 and 13). Thus the interaction between the cold pool and the warm moist air further enhances the system-scale vertical motion, yielding even stronger precipitation.

As shown in Sect. 4, the quasi-stationary MCS featured new convective developing from the rear of the convective line and propagating over the same region before the older convection completely disappeared. This process requires some initiation factors in order to continuously develop convection from the rear. This back-building convection coincided with the cold outflow boundary along the coastline at the intersection of the southwesterly LLJ with the outflow boundary. It can account for the southwestward advance of deep convection as a result of the interaction of moist air with convectively generated cold outflows (Weisman and Rotunno, 2004).

6 Summary and conclusions

This study presents an observational investigation of the extreme rainfall event over the southern Korean Peninsula on 7 July 2009. An extreme rainfall-producing quasi-stationary MCS produced record-breaking rainfall totals and devastating floods in Busan metropolitan area.

Synoptic and mesoscale analyses showed that extreme rainfall occurred north of the stationary Changma front. The southwesterly monsoonal flow transported warm and moist air, which glided up from the surface above the frontal slope. The advection of higher θ_e was also critical in the destabilization process as it promoted elevated convective instability over the sloping frontal zone. In the upper-level synoptic configuration, the trough and upper-level jet streak amplified the development of convection.

The important characteristic of the precipitation distribution is the much stronger rainfall observed over Busan. The extreme rainfall over Busan resulted from the continuous upstream initiation of deep convection (back-building process) at the coast. Moreover, the continuously developed convective cells moved parallel to older cells (i.e. training effect).

Understanding the back-building process requires accounting for mechanisms that lead to discrete convective updraft redevelopment and continuous updraft maintenance on the storm's upstream flank. Deep convection seen to the north of the convective line produced downdrafts containing cold and dense air that spread outward away from the convection. The outflow boundary on the southeastern periphery of the cold pool was a confluence between southwesterly and northeasterly flows. The unstable air mass and warm moist southwesterly LLJ over the upstream ocean combined to initiate new convection and provide a continuing source of moisture for the quasi-stationary MCS over Busan. Though the moist unstable air above convectively generated cold outflows can easily be lifted to produce precipitation, the upstream triggering of convection and a feed of warm moist air are important for a persistent MCS. Thus the quasi-stationary

Dominant processes of extreme rainfall-producing mesoscale convective system

J.-H. Jeong et al.

[Title Page](#)

[Abstract](#)

[Introduction](#)

[Conclusions](#)

[References](#)

[Tables](#)

[Figures](#)

[⏪](#)

[⏩](#)

[◀](#)

[▶](#)

[Back](#)

[Close](#)

[Full Screen / Esc](#)

[Printer-friendly Version](#)

[Interactive Discussion](#)

MCS could be responsible for the relatively long duration of convective events that led to the extreme rainfall over the Busan metropolitan area.

Acknowledgements. This research was funded by the Korea Meteorological Industry Promotion Agency under Grant KMIPA 2015-5060. This research was also supported by a grant from the National Institute of Fisheries Science (R2015053).

References

- Bluestein, H. B.: Principles of Kinematics and Dynamics, Vol. I, Synoptic-Dynamic Meteorology in Midlatitudes, Oxford University Press, Oxford, 329 pp., 1992.
- Bluestein, H. B. and Jain, M. H.: Formation of mesoscale lines of precipitation: severe squall lines in Oklahoma during the spring, *J. Atmos. Sci.*, 42, 1711–1732, 1985.
- Chappell, C. F.: Quasi-stationary convective events, in: *Mesoscale Meteorology and Forecasting*, edited by: Ray, P. S., Amer. Meteor. Soc., 289–309, 1986.
- Chen, G. T.-J. and Yu, C.-C.: Study of low-level jet and extremely heavy rainfall over northern Taiwan in the mei-yu season, *Mon. Weather Rev.*, 116, 884–891, 1988.
- Corfidi, S. F.: Cold pools and MCS propagation: forecasting the motion of downwind-developing MCSs, *Weather Forecast.*, 18, 997–1017, 2003.
- Corfidi, S. F., Merritt, J. H., and Fritsch, J. M.: Predicting the movement of mesoscale convective complexes, *Weather Forecast.*, 11, 41–46, 1996.
- Cressman, G. P.: An operational objective analysis system, *Mon. Weather Rev.*, 87, 367–374, 1959.
- Ding, Y.-H.: Summer monsoon rainfalls in China, *J. Meteorol. Soc. Jpn.*, 70, 337–396, 1992.
- Doswell III, C. A., Brooks, H. E., and Maddox, R. A.: Flash flood forecasting: an ingredients-based methodology, *Weather Forecast.*, 11, 560–581, 1996.
- Houze, R. A., Smull, B. F., and Dodge, P.: Mesoscale organization of springtime rainstorms in Oklahoma, *Mon. Weather Rev.*, 118, 613–654, 1990.
- Jeong, J.-H., Lee, D.-I., Wang, C.-C., Jang, S.-M., You, C.-H., and Jang, M.: Environment and morphology of mesoscale convective systems associated with the Changma front during 9–10 July 2007, *Ann. Geophys.*, 30, 1235–1248, doi:10.5194/angeo-30-1235-2012, 2012.

Dominant processes of extreme rainfall-producing mesoscale convective system

J.-H. Jeong et al.

[Title Page](#)

[Abstract](#)

[Introduction](#)

[Conclusions](#)

[References](#)

[Tables](#)

[Figures](#)

[I◀](#)

[▶I](#)

[◀](#)

[▶](#)

[Back](#)

[Close](#)

[Full Screen / Esc](#)

[Printer-friendly Version](#)

[Interactive Discussion](#)



Dominant processes of extreme rainfall-producing mesoscale convective system

J.-H. Jeong et al.

[Title Page](#)

[Abstract](#)

[Introduction](#)

[Conclusions](#)

[References](#)

[Tables](#)

[Figures](#)

[⏪](#)

[⏩](#)

[◀](#)

[▶](#)

[Back](#)

[Close](#)

[Full Screen / Esc](#)

[Printer-friendly Version](#)

[Interactive Discussion](#)

- Jeong, J. H., Lee, D.-I., Wang, C. C., Jang, S.-M., Park, S.-H., and Jung, S. A.: Structure and evolution of line-shaped convective systems associated with Changma front during GRL PHONE-09: 6 July 2009 case, *Meteorol. Appl.*, 21, 786–794, 2014.
- Junker, N. W., Schneider, R. S., and Fauver, S. L.: A study of heavy rainfall events during the Great Midwest Flood of 1993, *Weather Forecast.*, 14, 701–712, 1999.
- Kalnay, E., Kanamitsu, M., Kistler, R., Collins, W., Deavan, D., Gandin, L., Iredell, M., Saha, S., White, G., Woolen, J., Zhu, Y., Chelliah, M., Ebisuzaki, W., Higgins, W., Janowiak, J., Mo, K., Ropelewski, C., Wang, C., Leetmaa, J., Reynolds, A., Jenne, R., and Joseph, R., D.: The NCEP/NCAR 40-Year Reanalysis Project, *B. Am. Meteorol. Soc.*, 77, 437–472, 1996.
- Lee, D. K., Kim, H. R., and Hong, S. Y.: Heavy rainfall over Korea during 1980–1990, *Kor. J. Atmos. Soc.*, 1, 32–50, 1998.
- Lee, D. K., Park, J. G., and Kim, J. W.: Heavy rainfall events lasting 18 days from 31 July to 17 August 1998, over Korea, *J. Meteorol. Soc. Jpn.*, 86, 313–333, 2008.
- Li, J., Chen, Y.-L., and Lee, W.-C.: Analysis of a heavy rainfall event during TAMEX, *Mon. Weather Rev.*, 125, 1060–1082, 1997.
- Maddox, R. A., Chappell, C. F., and Hoxit, L. R.: Synoptic and meso-a scale aspects of flash flood events, *B. Am. Meteorol. Soc.*, 60, 115–123, 1979.
- NEMA – National Emergency Management Agency: *Yearly of Disasters*, 535 pp., 2009.
- Ninomiya, K.: Characteristics of Baiu front as a predominant subtropical front in the summer Northern Hemisphere, *J. Meteorol. Soc. Jpn.*, 62, 880–894, 1984.
- Ninomiya, K. and Akiyama, T.: Multi-scale features of Baiu, the summer monsoon over Japan and the East Asia, *J. Meteorol. Soc. Jpn.*, 70, 467–495, 1992.
- Orlanski, I.: A rational subdivision of scales for atmospheric processes, *B. Am. Meteorol. Soc.*, 56, 527–530, 1975.
- Park, S. U., Ahn, H. J., and Chun, Y. S.: Evolution of synoptic scale features associated with a long lived convective system (21–23 July 1987), *J. Korean Meteor. Soc.*, 25, 168–191, 1989.
- Parker, M. D. and Johnson, R. H.: Organizational modes of midlatitude mesoscale convective systems, *Mon. Weather Rev.*, 128, 3413–3436, 2000.
- Rotunno, R., Klemp, J. B., and Weisman, M. L.: A theory for strong, long-lived squall lines, *J. Atmos. Sci.*, 45, 463–485, 1988.
- Saito, K., Fujita, T., Yamada, Y., Ishida, J., Kumagai, Y., Aranami, K., Ohmori, S., Nagasawa, R., Kumagai, S., Muroi, C., Kato, T., Eito, H., and Yamazaki, Y.: The operational JMA nonhydrostatic mesoscale model, *Mon. Weather Rev.*, 134, 1422–1441, 2006.

Dominant processes of extreme rainfall-producing mesoscale convective system

J.-H. Jeong et al.

[Title Page](#)

[Abstract](#)

[Introduction](#)

[Conclusions](#)

[References](#)

[Tables](#)

[Figures](#)

[⏪](#)

[⏩](#)

[◀](#)

[▶](#)

[Back](#)

[Close](#)

[Full Screen / Esc](#)

[Printer-friendly Version](#)

[Interactive Discussion](#)



Sampe, T. and Xie, S.-O.: Large-scale dynamics of the Meiyu–Baiu rainband: environmental forcing by the westerly jet, *J. Climate*, 23, 113–134, 2010.

Schumacher, R. S. and Johnson, R. H.: Organization and environmental properties of extreme-rain-producing mesoscale convective systems, *Mon. Weather Rev.*, 133, 961–976, 2005.

5 Schumacher, R. S. and Johnson, R. H.: Mesoscale processes contributing to extreme rainfall in a midlatitude warm-season flash flood, *Mon. Weather Rev.*, 136, 3964–3986, 2008.

Sun, J. and Lee, T. Y.: A numerical study of an intense quasi-stationary convection band over the Korean Peninsula, *J. Meteorol. Soc. Jpn.*, 80, 1221–1245, 2002.

10 Trier, S. B., Davis, C. A., Ahijevych, D. A., Weisman, M. L., and Bryan, G. H.: Mechanisms supporting long-lived episodes of propagating nocturnal convection within a 7-day WRF model simulation, *J. Atmos. Sci.*, 63, 2437–2461, 2006.

Uccellini, L. W.: Processes contributing to the rapid development of extratropical cyclones, in: *Extratropical Cyclones: The Erik Palmén Memorial Volume*, edited by: Newton, C. W. and Holopainen, E. O., *Amer. Meteor. Soc.*, 81–105, 1990.

15 Uccellini, L. W. and Johnson, D. R.: The coupling of upper- and lower-tropospheric jet streaks and implications for the development of severe convective storms, *Mon. Weather Rev.*, 107, 682–703, 1979.

Wang, C.-C., Chen, G. T.-J., and Huang, S.-Y.: Remote trigger of deep convection by cold outflow over the Taiwan Strait in the mei-yu season: a modeling study of the 8 June 2007 case, *Mon. Weather Rev.*, 139, 2854–2875, 2011.

20 Wang, C.-C., Chen, G. T.-J., Huang, H.-L., Carbone, R. E., and Chang, S.-W.: Synoptic conditions associated with propagating and nonpropagating cloud/rainfall episodes during the warm season over the East Asian continent, *Mon. Weather Rev.*, 140, 721–747, 2012.

25 Weisman, M. L. and Rotunno, R.: “A theory for strong long-lived squall lines” revisited, *J. Atmos. Sci.*, 61, 361–382, 2004.

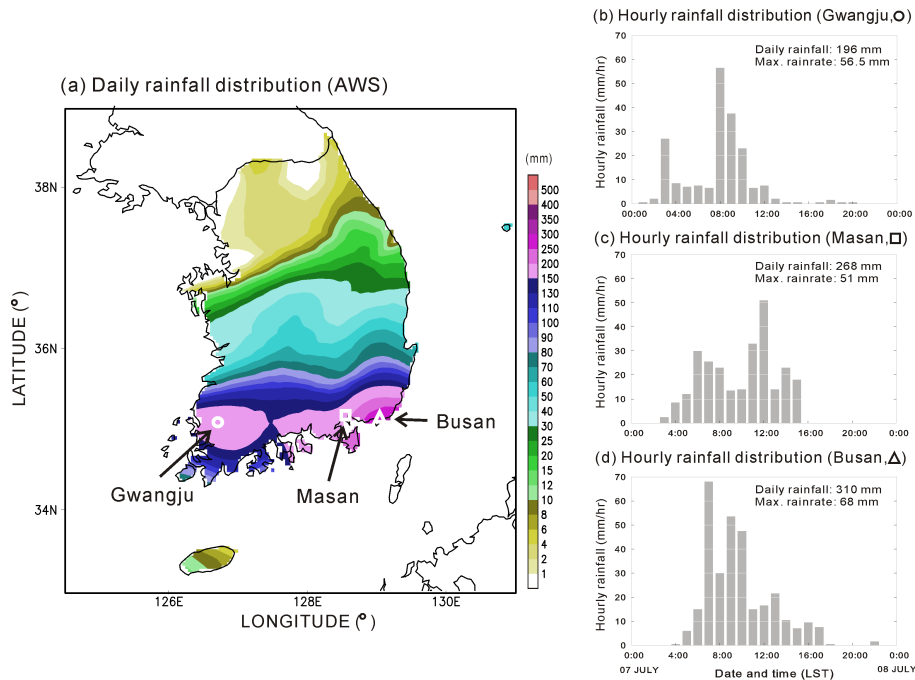


Figure 2. (a) The 24 h accumulated rainfall amounts in Korea on 7 July 2009. The locations of the three weather stations are shown. Hourly rainfall distribution at (b) Gwangju, (c) Masan, and (d) Busan.

[Title Page](#)

[Abstract](#) [Introduction](#)

[Conclusions](#) [References](#)

[Tables](#) [Figures](#)

[⏪](#) [⏩](#)

[◀](#) [▶](#)

[Back](#) [Close](#)

[Full Screen / Esc](#)

[Printer-friendly Version](#)

[Interactive Discussion](#)



**Dominant processes
of extreme
rainfall-producing
mesoscale
convective system**

J.-H. Jeong et al.

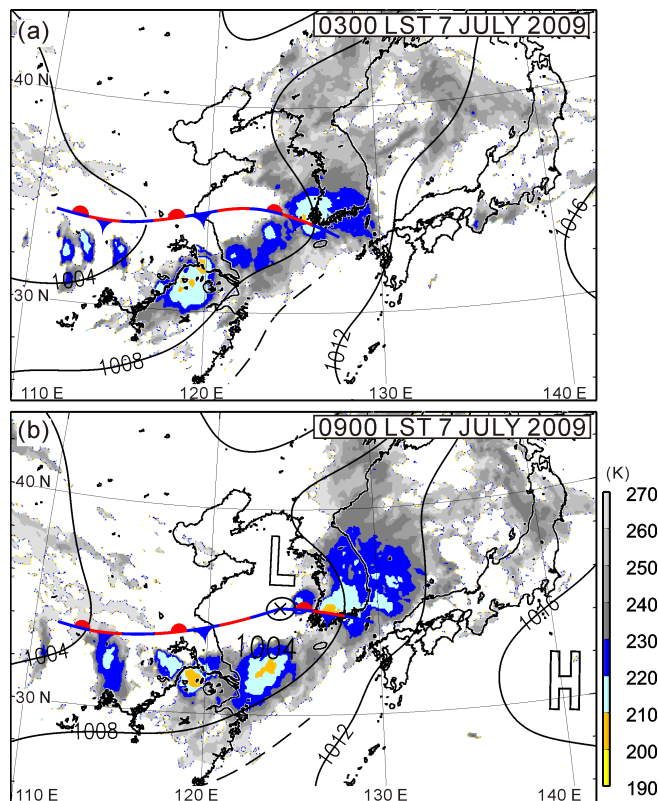


Figure 3. Surface weather maps with superimposed MTSAT-IR images (color shading) at (a) 03:00 LST and (b) 09:00 LST 7 July 2009.

Dominant processes of extreme rainfall-producing mesoscale convective system

J.-H. Jeong et al.

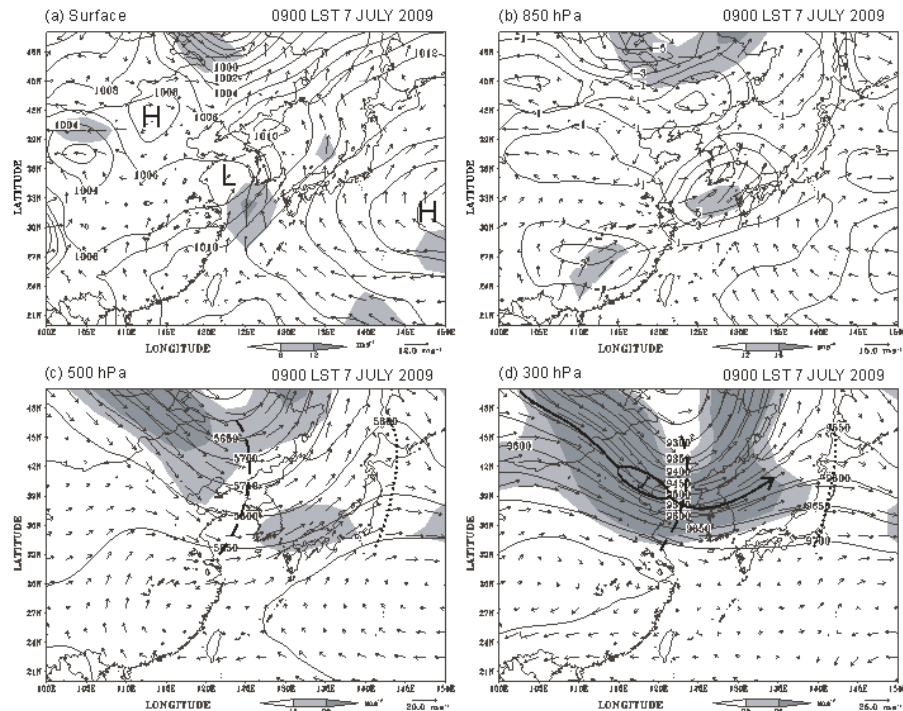


Figure 4. NCEP–NCAR reanalysis of **(a)** horizontal wind vectors (ms^{-1} , speed also shaded) and pressure (hPa, contours) at mean sea level, **(b)** horizontal wind vectors (ms^{-1} , shaded), temperature advection (10^{-2}K s^{-1} , contours) at 850 hPa, and **(c)–(d)** horizontal wind vectors (ms^{-1} , shaded), and geopotential height (gpm, contour every 50 gpm) at **(c)** 500 and **(d)** 300 hPa for 09:00 LST 7 July 2009. Thick dashed (dotted) lines in **(c)–(d)** depict the trough (ridge), and the core and axis of the upper-level jet (ULJ) are also marked in **(d)**.

[Title Page](#)
[Abstract](#)
[Introduction](#)
[Conclusions](#)
[References](#)
[Tables](#)
[Figures](#)
[Back](#)
[Close](#)
[Full Screen / Esc](#)
[Printer-friendly Version](#)
[Interactive Discussion](#)

Dominant processes of extreme rainfall-producing mesoscale convective system

J.-H. Jeong et al.

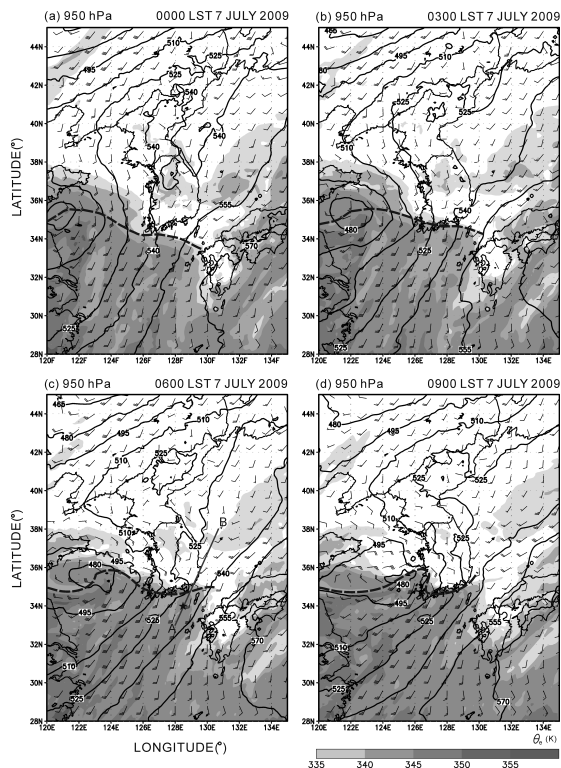


Figure 5. Mesoscale analysis of horizontal winds (ms^{-1} , barbs), geopotential height (gpm, solid contours), and equivalent potential temperature (θ_e , K, shaded) at 950 hPa for **(a)** 00:00, **(b)** 03:00, **(c)** 06:00, and **(d)** 09:00 LST 7 July 2009. Contour intervals are 15 gpm for geopotential height, and full (half) barbs represent winds of 5 (2.5) ms^{-1} . The location of the front is also plotted as a dashed line. In **(c)** the line A–B shows the location of the vertical cross section used in Fig. 6 and the asterisk at 34°N , 128.5°E depicts the sounding location shown in Fig. 7.

[Title Page](#)
[Abstract](#)
[Introduction](#)
[Conclusions](#)
[References](#)
[Tables](#)
[Figures](#)
[Back](#)
[Close](#)
[Full Screen / Esc](#)
[Printer-friendly Version](#)
[Interactive Discussion](#)

Dominant processes of extreme rainfall-producing mesoscale convective system

J.-H. Jeong et al.

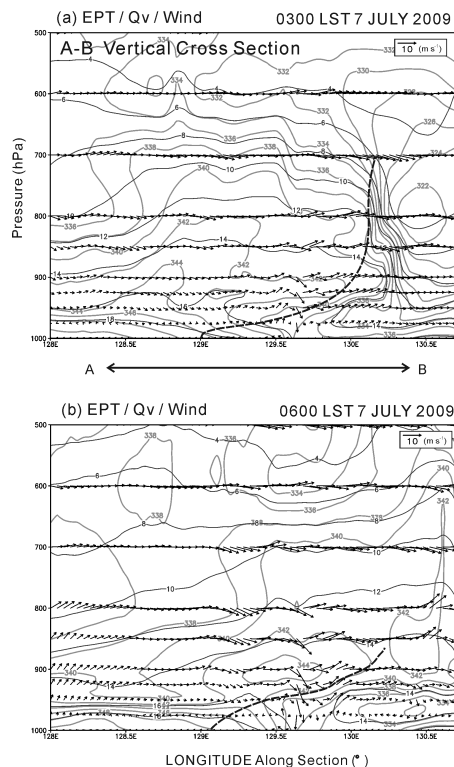


Figure 6. Vertical cross sections from 128° E, 33° N to 131° E, 38° N (transect A–B in Fig. 5c) of equivalent potential temperature (θ_e , K, gray line), specific humidity (q , g kg^{-1} , black line), and wind vectors (m s^{-1}) along the section plane between 1000 and 500 hPa at **(a)** 03:00 and **(b)** 06:00 LST 7 July 2009. The thick dashed lines indicate the frontal zone. Contour intervals are 2 K for θ_e and 2 g kg^{-1} for q .

Title Page

Abstract

Introduction

Conclusions

References

Tables

Figures

◀

▶

◀

▶

Back

Close

Full Screen / Esc

Printer-friendly Version

Interactive Discussion

Dominant processes of extreme rainfall-producing mesoscale convective system

J.-H. Jeong et al.

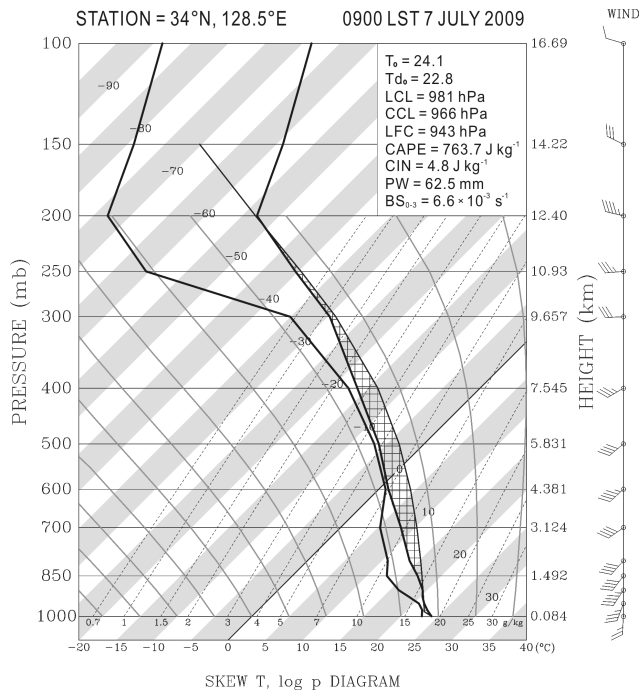


Figure 7. Skew T–log p plot of vertical profiles of temperature, dew-point temperature, and horizontal wind (ms^{-1}) at 34° N, 128.5° E (cf. Fig. 5b for location) at 09:00 LST 7 July 2009 in the simulation. The process curve for a surface air parcel is plotted. For winds, full (half) barbs denote 5 (2.5 ms^{-1}).

[Title Page](#)

[Abstract](#)

[Introduction](#)

[Conclusions](#)

[References](#)

[Tables](#)

[Figures](#)

[◀](#)

[▶](#)

[◀](#)

[▶](#)

[Back](#)

[Close](#)

[Full Screen / Esc](#)

[Printer-friendly Version](#)

[Interactive Discussion](#)



**Dominant processes
of extreme
rainfall-producing
mesoscale
convective system**

J.-H. Jeong et al.

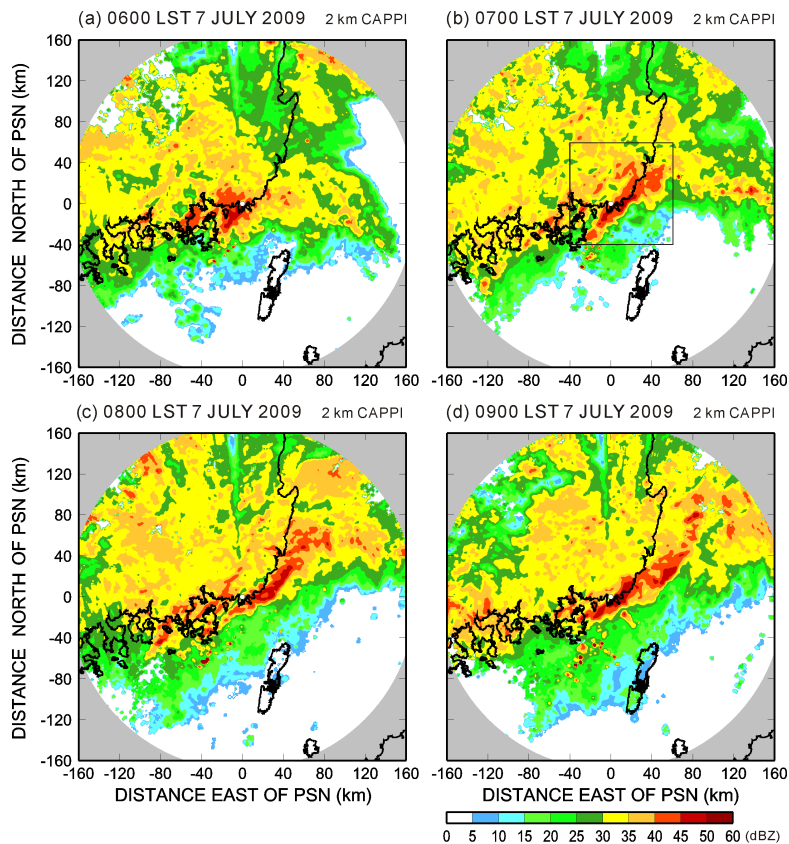


Figure 8. Horizontal section of radar reflectivity (dBZ, color shading) at a height of 2 km observed by PSN radar at hourly intervals from (a) 06:00 to (d) 09:00 LST 7 July 2009. The box in (b) indicates the domain for Fig. 9.

Dominant processes of extreme rainfall-producing mesoscale convective system

J.-H. Jeong et al.

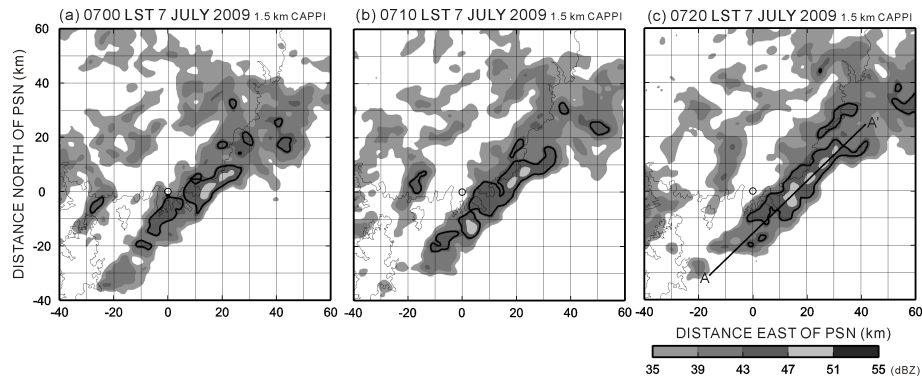


Figure 9. Horizontal section of radar reflectivity (dBZ, shading) at a height of 2 km observed by PSN the radar at 10 min intervals from (a) 07:00 LST to (c) 07:20 LST 7 July 2009. The contour denotes 45 dBZ. In (c) the line A–A' shows the location of the vertical cross section used in Fig. 10.

[Title Page](#)[Abstract](#)[Introduction](#)[Conclusions](#)[References](#)[Tables](#)[Figures](#)[⏪](#)[⏩](#)[◀](#)[▶](#)[Back](#)[Close](#)[Full Screen / Esc](#)[Printer-friendly Version](#)[Interactive Discussion](#)

Dominant processes of extreme rainfall-producing mesoscale convective system

J.-H. Jeong et al.

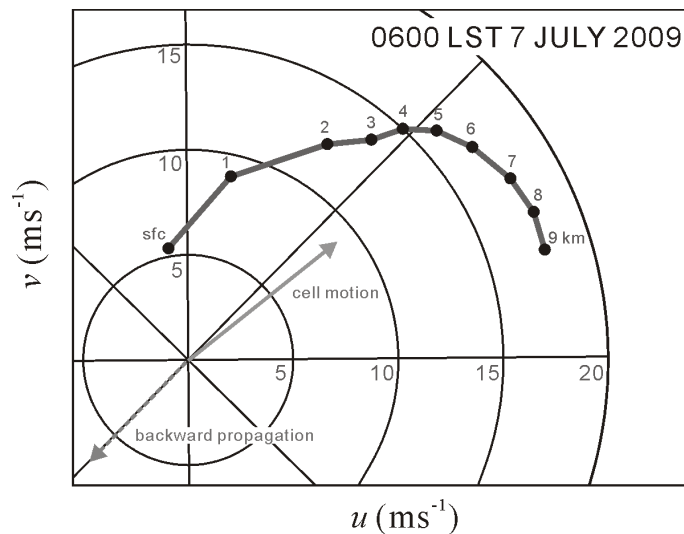


Figure 11. Hodograph computed using JMA-MSM gridded analyses averaged over the domain $33.7\text{--}36.4^\circ\text{ N}$, $127.4\text{--}130.7^\circ\text{ E}$ (cf. Fig. 1) at 06:00 LST 7 July 2009. The gray vectors denote the direction and speed of cell motion (dashed line) and backward propagation (solid line), respectively.

[Title Page](#)
[Abstract](#)
[Introduction](#)
[Conclusions](#)
[References](#)
[Tables](#)
[Figures](#)
[⏪](#)
[⏩](#)
[◀](#)
[▶](#)
[Back](#)
[Close](#)
[Full Screen / Esc](#)
[Printer-friendly Version](#)
[Interactive Discussion](#)

Dominant processes of extreme rainfall-producing mesoscale convective system

J.-H. Jeong et al.

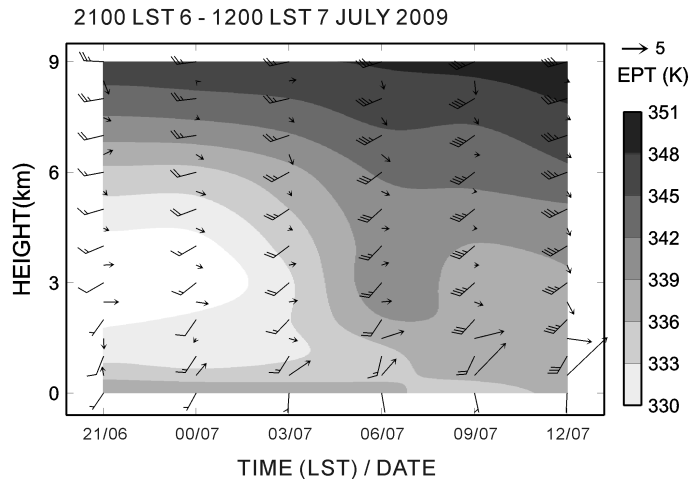


Figure 12. Time–height diagram of horizontal winds [m s^{-1} , barbs, full (half) barbs denote 5 (2.5) m s^{-1}], vertical wind shear vectors (10^{-5} s^{-1}), and equivalent potential temperature (θ_e , K, shaded), computed as for Fig. 11 from 21:00 LST 6 to 12:00 LST 7 July 2009.

[Title Page](#)

[Abstract](#)

[Introduction](#)

[Conclusions](#)

[References](#)

[Tables](#)

[Figures](#)

[⏪](#)

[⏩](#)

[◀](#)

[▶](#)

[Back](#)

[Close](#)

[Full Screen / Esc](#)

[Printer-friendly Version](#)

[Interactive Discussion](#)

Dominant processes of extreme rainfall-producing mesoscale convective system

J.-H. Jeong et al.

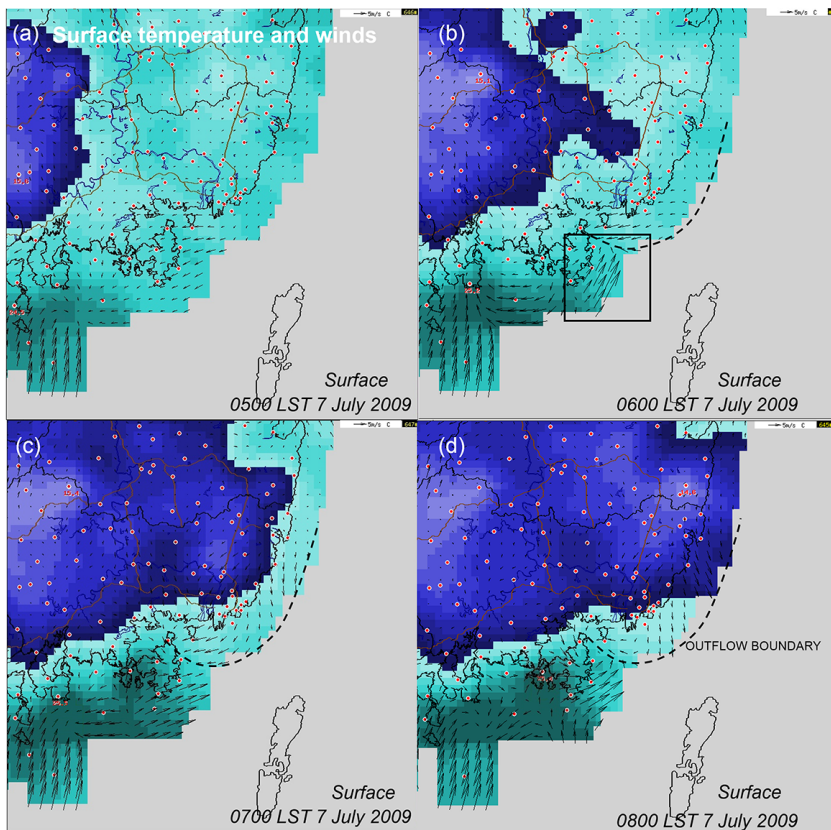


Figure 13. Surface temperature ($^{\circ}\text{C}$, color shading) and wind vectors (m s^{-1}) at (a) 05:00, (b) 06:00, (c) 07:00, and (d) 08:00 LST 7 July 2009. The position of the outflow boundary is denoted by a dashed black line.